Enhanced reflectivity of backthrusts in the recent great Sumatran earthquake rupture zones

S. C. Singh, N. D. Hananto, A. P. S. Chauhan

Enhanced reflectivity of backthrusts in the recent great Sumatran earthquake rupture zones

S. C. Singh,[1] N. D. Hananto,[1] and A. P. S. Chauhan[1]

Received 18 November 2010; revised 28 December 2010; accepted 6 January 2010; published 16 February 2011.

[1] In the last five years, there have been three great megathrust earthquakes in the Sumatra subduction zone, and a part of the zone is still locked. We have carried out deep seismic reflection surveys along the SW Sumatran margin and have imaged backthrusts along four profiles down to 15–20 km depth. We find that the seismic images of the backthrusts in the 2004 and 2007 great earthquake ruptured zones are brighter than those in the regions where the subduction zone is still locked. We suggest that this enhanced reflectivity is due to the increase of fluid contents along the reactivated backthrusts during or soon after the great earthquakes. If this interpretation is valid, then the backthrusts observed in the forearc basins could be used to monitor fluid movement from mantle wedge and earthquake precursors before and after an imminent great earthquake in the Sumatra locked zone. **Citation:** Singh, S. C., N. D. Hananto, and A. P. S. Chauhan (2011), Enhanced reflectivity of backthrusts in the recent great Sumatran earthquake rupture zones, *Geophys. Res. Lett.*, *38*, L04302, doi:10.1029/2010GL046227.

1. Introduction

[2] The great earthquakes occur on megathrusts, the interface between the subducting downgoing plate and the overriding plate, rupturing the seismogenic zone, which generally lies between 10 and 30 km depths beneath the forearc. The overriding plate beneath the forearc region consists of accreted sediments and crystalline crust with a backstop boundary between them. Although the megathrust position has been imaged using different techniques [*Singh et al.*, 2008; *Dessa et al.*, 2009], it has been rather difficult to image the backstop position [*Bangs et al.*, 2003; *Trehu et al.*, 1994] because of the poor penetration of seismic energy beneath thick accreted sediments, strong scattering from rough seafloor, reverberation of seismic energy (multiples) in the water column, and steep dips. Using a state of the art industry technology, we have recently been able to image the backthrusts down to 20 km depth in the Sumatran subduction zone [*Chauhan et al.*, 2009].

[3] In the Sumatra subduction zone, the Indo-Australian plate subducts beneath the Sunda plate obliquely with a convergence rate varying from 60 mm/yr in the south to 52 mm/yr in northern Sumatra [*Prawirodirdjo and Bock*, 2004]. The Sumatra subduction zone has been seismically very active in the recent past, which started on December 26, 2004 with the Mw = 9.2 earthquake that produced a devastating tsunami in the Indian Ocean region [*Subarya et al.*, 2006]. The main earthquake was the biggest such event in the last forty years and broke 1300 km of the plate boundary from Simeulue Island all the way to Andaman Islands (Figure 1). A second megathrust earthquake of magnitude Mw = 8.7 occurred on March 28, 2005, 150 km further SE of the December 2004 event breaking 350 km of the plate boundary between Simeulue and Nias Islands [*Briggs et al.*, 2008]. After a couple of years of quiescence, a magnitude 8.4 earthquake occurred near Bengkulu on September 12, 2007, at 1300 km SE of the December 2004 event, breaking 200 km of the plate boundary [*Konca et al.*, 2008] and leaving a gap of about 600 km between the 2005 and 2007 events (Figure 1) [*Sieh et al.*, 2008]. A part of this patch ruptured on October 25, 2010 with Mw = 7.8, producing tsunami up to 8 m high on SW coast of Pagai Islands. There is a weakly coupled (aseismic) zone SE of the 2007 earthquake region [*Chlieh et al.*, 2008]. In the last four years, we have carried out two deep seismic reflection surveys in the earthquake ruptured as well as in the locked and aseismic zones in partnership with industry; here we present results from these two surveys with a special emphasis on the role of backthrusts.

2. Seismic Reflection Survey

[4] We acquired five deep seismic reflection profiles covering about 1300 km of the Sumatra subduction margin (Figure 1). Two profiles (WG1 and WG2) were shot in the 2004 earthquake epicentral region and three in the 2007 earthquake and Sumatra seismic and aseismic regions (CGGV010, CGGV020, CGGV040) [*Chlieh et al.*, 2008; *Singh et al.*, 2009]. Profiles WG1 and WG2 were acquired by WesternGeco in July 2006 on board the seismic vessel Geco Searcher towing a 12-km-long streamer at 15 m water depth and a 10700 cubic-inch airgun source at 15 m depth [*Singh et al.*, 2008]. CGGV profiles were acquired by CGGVeritas in May 2009 on board the seismic vessel Geowave Champion towing a 15-km-long streamer at 22.5 m depth, the longest streamer ever used, and a 9600 cubic inch airgun source at 15 m depth [*Singh et al.*, 2009]. The shot spacing was 50 m and record length was 20 s. The data were resampled to 8 ms and filtered using 2-45 Hz anti-alias filter. An iterative interactive velocity analysis was used in combination with 4–6 passes of radon multiple removal technique [*Verschuur et al.*, 1992] to enhance the image of deeper reflections. The data were migrated using 2D ray-based Kirchhoff post-stack time migration technique using a smoothed version of the velocity obtained for stacking. The whole data acquisition and processing techniques were optimised to image the deep structure of the subduction system down to 45 km depth [*Singh et al.*, 2008].

[1]Equipe de Geosciences Marines, Institut de Physique du Globe de Paris, Paris, France.

0094-8276/11/2010GL046227

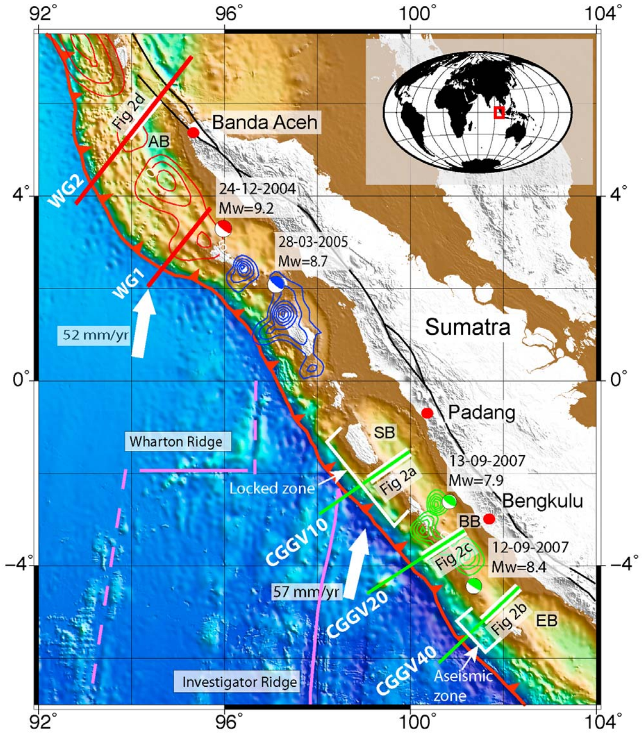

Figure 1. Bathymetric map derived from GEBCO data. The 2004 earthquake location is indicated by red beach ball, 2005 with blue and 2007 with green beach balls. The colour contours are the co-seismic slip during the great earthquakes [*Konca et al.*, 2008; *Chlieh et al.*, 2007]. Thin red lines (WG1 and WG2) are seismic profiles acquired by WesternGeco and thin green lines (CGGV010, CGGV020, CGGV040) are acquired by CGGVeritas. Thick white lines are the part of the data shown in Figure 2. AB: Aceh Basin, SB: Siberut Basin, BB: Bengkulu Basin, EB: Engano Basin.

[5] Most of the profiles are 240 km long and traverse the whole subduction system from the subducting oceanic plate on the Indo-Australian plate, subduction front, accretionary wedge, forearc high and forearc basin. Here, we present results from the forearc high, which is the submerged part of Mentawai-Andaman Islands, and the forearc basins that separate mainland Sumatra from the Islands. Figure 2 shows interpreted seismic reflection images along four profiles as a function of two-way travel time (TWTT).

3. Seismic Results

[6] Figure 2a is along the locked portion of the Sumatra seismic gap [*Chlieh et al.*, 2008] (CGGV010), which traverses the Siberut Basin, which is 1700 m deep. The sediment thickness in the Siberut forearc basin increases from 1 s (1 km) TWTT to 4 s TWTT (4–5 km). The basement is clearly imaged. At the centre of the basin two branches of seaward dipping backthrust are clearly imaged that control the formation of the piggyback basin previously imaged by *Singh et al*. [2010] using shallow seismic reflection profiling. Landward dipping thrusts are imaged on the SW margin of the forearc high. The top of the oceanic plate is clearly imaged at 10–13 s TWTT. The oceanic Moho is visible along a part of the profile. A weak sub-horizontal reflection is imaged at 11 s TWTT, probably from the continental Moho. A weak seaward reflection is observed at 8 s TWTT beneath the forearc high, which might be the continuation of the backthrust at depth.

[7] Profile CGGV040 (Figure 2b) is at 50 km south of the 2007 earthquake epicentre, in the aseismic zone [*Chlieh et al.*, 2008] and traverses the Engano Basin, which is also 1700 m deep. The sedimentary structure in the Engano forearc basin is similar to that in the Siberut basin, with two push-up ridges, suggesting a transpressional regime, which is possibly connected with a seaward dipping backthrust beneath the forearc high. SW margin of the forearc high is bounded by a landward dipping thrust. Both the top and bottom of the subducting oceanic crust are clearly imaged along the profile. A weak reflection at 11 s TWTT corresponds to the continental Moho.

[8] Figure 2c shows seismic image across the 2007 earthquake rupture zone where maximum slip occurred [*Konca et al.*, 2008] (CGGV020). The Bengkulu Basin is shallow at 1100 m water depth. The maximum sediment thickness is 5 s along this profile. The complex nature of the push-up ridge suggests the presence of a strike-slip fault with some thrust component of motion. A strong reflector is imaged beneath the forearc high that continues down to 8 s TWTT close to the oceanic plate, and is a continuation of the basement or the backthrust. Both the top and bottom of the oceanic crust are imaged along a part of the profile. If we project the epicentre of the 2007 earthquake, it will be around 10 s TWTT at CMP 4500.

[9] Figure 2d shows the seismic profile across the 2004 great Sumatra earthquake rupture zone [*Chlieh et al.*, 2007]. The forearc basin here is narrow (25 km wide) at 2000 m water depth and is bounded by the Sumatra continental crust in the NE. The maximum sediment thickness is 1.5 s. The shallowest part of the forearc high is at 300 m water depth and capped by a 1–1.5 s TWTT folded and faulted sediments, suggesting that it has been uplifted. The NE margin of the forearc high is bounded by two strong reflections that penetrate down to 9 s TWTT. Using tomographic results, *Chauhan et al.* [2009] suggest that these reflectors correspond to active backthrust and continental backstop. There are some weak reflections on the southwest side of the forearc high, which might be a conjugate fault bounding the forearc ridge. The top of the oceanic plate is clearly imaged at 11–14 s TWTT. The weak reflection at 11 s is the continental Moho [*Chauhan et al.*, 2009; *Singh et al.*, 2008]. The projection of the 2004 great Sumatra earthquake is at 12.5 s TWTT at CMP 29850.

[10] It is interesting to note that the backthrusts are strongly reflective in the 2004 and 2007 earthquakes ruptured zones (Figures 2c and 2d) but it is very weak in the locked (Figure 2a) and aseismic zones (Figure 2b). On profile CGGV020, the backthrust is imaged down to the plate interface but on profile WG2 it is imaged down to 9 s only, which could be due to poor imaging conditions at depth, particularly due to steep dip of the backthrust near the plate interface. Since we have used similar acquisition and processing techniques for all the profiles, the difference in the reflectivity seems to be real. Although the dominant frequencies of the backthrust reflections are slightly different in two surveys, 5–6 Hz in the CGGVeritas survey and 8–10 Hz in the WesternGeco survey, the enhanced reflectivity is

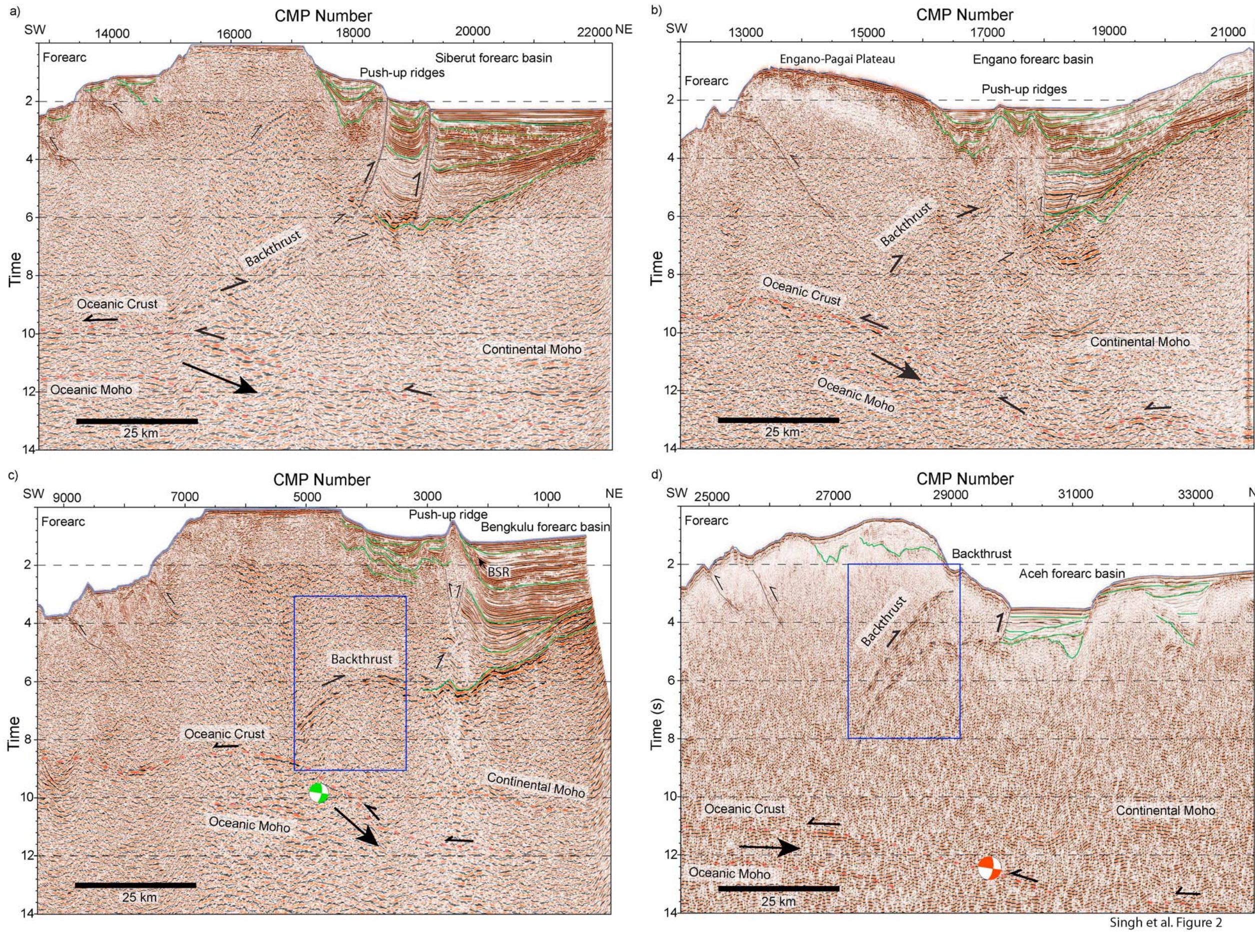

Figure 2. Interpreted Seismic profiles: Two seismic profiles (a) CGGV010 and (b) CGGV040 are in the region where there has been no great earthquakes for the last 200 years [*Sieh et al.*, 2008] and (c and d) two profiles WG2 and CGGV020 traverse the maximum rupture zones of 2004 and 2007 earthquakes. Green curves indicate sedimentary strata, dashed red oceanic crust and brown continental Moho. Dashed black: backthrust, thin solid black: near surface faults. Blue rectangles outline the images shown in Figure 3. The beach balls indicate the projection of the 2007 (green) and 2004 (red) hypocentres along the seismic profiles. Vertical to horizontal ratio is 1:8.

observed in the 2004 and 2007 earthquake rupture zones only (Figure 3). The complex seafloor topography and dip of the reflector do not lend themselves to advanced inversion techniques [*Singh et al.*, 1998]. The polarity of the reflector is complex, and therefore it is difficult to say if the reflection is from a positive or negative velocity contrast (Figure 3). However, we have computed the ratio of the reflection amplitudes of backthrust and seafloor, which is 0.2 in the 2004 and 2007 earthquake ruptured zones and 0.02–0.05 for the locked and aseismic zones, suggesting an enhancement of the backthrust amplitude by a factor 5–10 in the recently ruptured zone.

4. Discussion and Conclusions

[11] *Chauhan et al.* [2009] have suggested that the backthrust imaged on profile WG2 (Figure 2) is active and might have slipped co-seismically during the 2004 earthquake and enhanced the tsunami in the Banda Aceh area. Using shallow seismic reflection and bathymetric data, *Singh et al*. [2010] have imaged backthrusts all along the NE margin of Siberut-Pagai islands. Therefore, the enhanced reflectivity of backthrusts at depth in the recently ruptured section of the Sumatra subduction margin is likely to be due to reactivated backthrust during or soon after the great earthquakes. However, we cannot rule out the possible role of lithology across the interface in the enhancement of reflectivity.

[12] Reactivated backthrusting would permit fluid flow along the fault surface and hence enhance the reflectivity of the backthrust. Since fluids at the plate interface are generally in an over-pressured condition they are likely to be expulsed during an earthquake and flow upwards along the steeply dipping backthrust (Figure 4). As the reactivated backthrust is close to the mantle wedge (within 10 km) as compared to the thrusts at the subduction front (100 km) (Figure 4), it may provide an easy pathway for fluids from the serpentinized mantle wedge region to the seafloor. The 2004 earthquake-rupture initiated below the forearc mantle [*Singh et al.*, 2008; *Dessa et al.*, 2009]. Similarly, the second of 2007 earthquake was below the forearc mantle [*Konco et al.*, 2008]. Therefore, it is possible that the

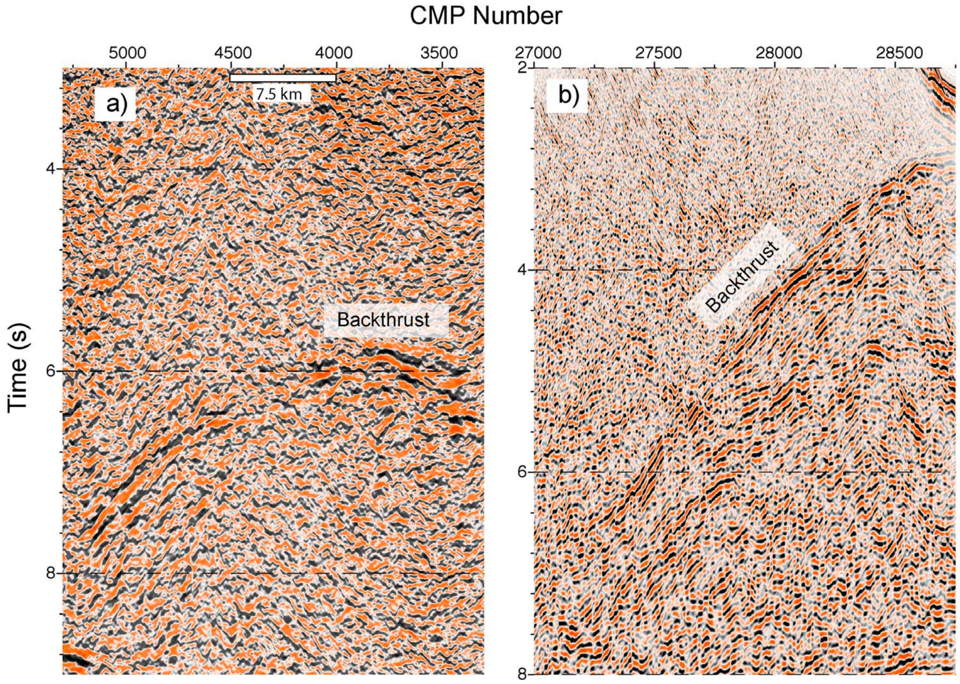

Figure 3. Blow-up of seismic reflection images of backthrusts along profiles WG2 and CGGV020 showing enhanced reflectivity down to 8 s two-way travel time.

enhanced reflectivity of the backthrusts observed on our seismic profiles could be due to mantle-derived fluid during or after these earthquakes. If this is the case, seismic reflection images could be used as a proxy for reactivated backthrusts and recent fluid flow after megathrust earthquakes.

[13] Serpentine mud-diapirs have been observed in other subduction systems (Marianas forearc region, Barbados accretionary wedge) [*Maekawa et al.*, 1993; *Fryer et al.*, 1990; *Brown and Westbrook*, 1988], and mud-diapirs resulting from mud channelled along backthrust branches have been reported in the Mediterranean accretionary wedge south of Crete [*Kopf*, 2002]. In the Marianas arc region, mud volcanoes have been observed between 45 and 90 km distance from the trench axis, contain traces of serpentinite clasts of mantle wedge origin and are associated with deep-rooted faults [*Hulme et al.*, 2010]. Mud diapirs containing melange are also present on Siberut and Nias Islands, suggestive of fluids originating at a great depth [*Samuel and Harbury*, 1996]. The push-up ridges in the forearc basin we have observed are 125 km from the subduction front and are associated with deep rooted active faults, and hence are likely to be influenced by fluid flow from the mantle wedge. The complex structures of the push-up ridges and the poor seismic reflectivity underneath indicate the presence of some other processes, such as fluid flow, along with tectonic processes (faulting). Although poorly constrained, the average P-wave velocity in the mantle wedge is 7.5 km/s along profile WG2, lower than the normal mantle velocity of 8 km/s [*Chauhan*, 2010], suggestive of serpentinized mantle wedge.

[14] On profile CGGV020, there is a bottom simulating reflector (BSR) around the push-up ridge (Figure 2c), which is generally associated with methane hydrate stability zone; this reflector corresponds to a thin layer of free methane [*Singh et al.*, 1993]. Although BSRs are generally linked to methane of thermogenic and biogenic origins, it is possible that the BSR on profile CGGV020 is due increase of gas content during the 2007 earthquake and might contain mantle-derived methane produced by serpentinization pro-

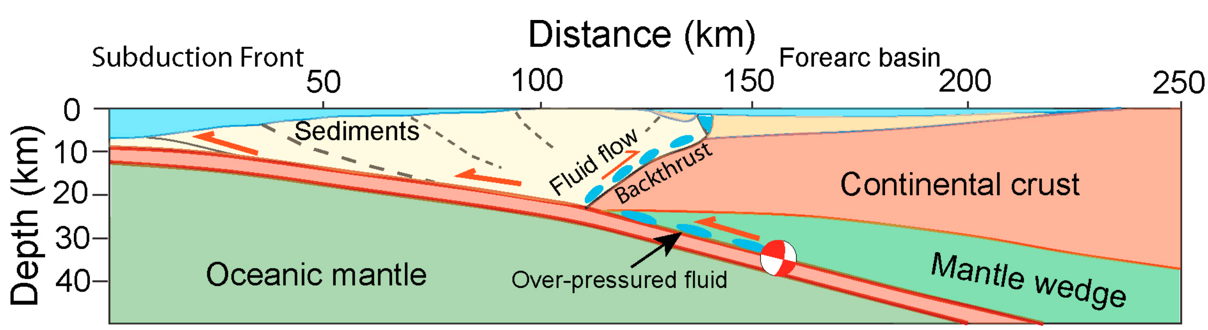

Figure 4. Schematic diagram showing the position of megathrust (thick red arrow), backthrust (thin red arrow) and fluid flow path (blue ellipse). The brown-white beach ball indicates a position of megathrust earthquake.

cess [*Fryer at al.*, 2000]. High methane content in pore fluids was detected at site 789 on ODP Leg 125 [*Fryer et al.*, 1990] in Marianas serpentine seamount. It would be easier to drill holes (1–1.5 km) in shallow waters of the forearc basin as compared to near the subduction front at 4.5–6 km water depth. Being closer to forearc islands, these sites are an ideal place for monitoring of fluid flow prior to and after large earthquakes in the Sumatra Seismic gap region [*McCloskey et al.*, 2010]. Seismic images along with other geophysical and geochemical observations (monitoring) before, during, and after an imminent megathrust earthquake would be a unique opportunity to unravel the complex processes of great earthquakes and tsunami generations.

[15] **Acknowledgments.** The seismic reflection data acquisition and processing were funded by WesternGeco and CGGVeritas. This is an IPG Paris contribution number 3123.

References

Bangs, N. L., G. L. Christenson, and T. H. Shipley (2003), Structure of the Lesser Antilles subduction zone backstop and its role in a large accretionary system, *J. Geophys. Res.*, *108*(B7), 2358, doi:10.1029/2002JB002040.

Briggs, R. W., et al. (2008), Deformation and slip along the Sunda Megathrust in the great 2005 Nias-Simeulue earthquake, *Science*, *311*, 1897–1901.

Brown, K., and G. K. Westbrook (1988), Mud diapirism and subcretion in the Barbados ridge accretionary complex: The role of fluids in accretionary processes, *Tectonics*, *7*, 613–640.

Chauhan, A. P. S. (2010), Structure of the northern Sumatra subduction megathrust using seismic reflection and refraction data, Ph.D. thesis, Institut de Physique du Globe de Paris, Paris.

Chauhan, A. P. S., et al. (2009), Seismic imaging of forearc backthrusts at northern Sumatra subduction zone, *Geophys. J. Int.*, *179*, 1772–1780.

Chlieh, M., et al. (2007), Coseismic slip and afterslip of the great Mw 9.15 Sumatra-Andaman earthquake of 2004, *Bull. Seismol. Soc. Am.*, *97*(1A), S152–S173.

Chlieh, M., J.-P. Avouac, K. Sieh, D. H. Natawidjaja, and J. Galetzka (2008), Heterogeneous coupling of the Sumatran megathrust constrained by geodetic and paleogeodetic measurements, *J. Geophys. Res.*, *113*, B05305, doi:10.1029/2007JB004981.

Dessa, J.-X., et al. (2009), Megathrust earthquakes can nucleate in the forearc mantle: Evidence from the 2004 Sumatra event, *Geology*, *37*, 659–662.

Fryer, P., K. L. Saboda, L. E. Johnson, M. E. MacKay, G. F. Moore, and P. Stoffers (1990), Conical seamount: Sea-MARC II, Alvin submersible, and seismic reflection studies, *Proc. Ocean Drill. Program Initial Rep.*, *125*, 5–14.

Fryer, P., J. P. Lockwood, N. Becker, S. Phipps, and C.S. Todd (2000), Significance of serpentine mud volcanism in convergent margins, in *Ophiolites and Oceanic Crust*, edited by Y. Dilek and E. Moore, *Spec. Publ. Geol. Soc. Am.*, 349, 35–51.

Hulme, S. M., C. G. Wheat, P. Fryer, and M. J. Mottl (2010), Pore water chemistry of the Mariana serpentinite mud volcanoes: A window to the seismogenic zone, *Geochem. Geophys. Geosyst.*, *11*, Q01X09, doi:10.1029/2009GC002674.

Konca, A. O., et al. (2008), Partial rupture of a locked patch of the Sumatra megathrust during the 2007 earthquake sequence, *Nature*, *456*, 631–635.

Kopf, A. J. (2002), Significance of mud volcanism, *Rev. Geophys.*, *40*(2), 1005, doi:10.1029/2000RG000093.

Maekawa, H., M. Shozui, T. Ishii, P. Fryer, and J. A. Pearce (1993), Blueschist metamorphism in an active subduction zone, *Nature*, *364*, 520–523, doi:10.1038/364520a0.

McCloskey, J., D. Lange, F. Tilmann, S. Nalbant, A. Bell, D. Natawidjaja, and A. Rietbrock (2010), The September 2009 Padang earthquake, *Nat. Geosci.*, *3*, 70–71.

Prawirodirdjo, L., and Y. Bock (2004), Instantaneous global plate motion model from 12 years of continuous GPS observations, *J. Geophys. Res.*, *109*, B08405, doi:10.1029/2003JB002944.

Samuel, M. A., and N. A. Harbury (1996), The Mentawai fault zone and deformation of the Sumatra foreac in Nias area, in *Tectonic Evolution of Southeast Asia*, edited by R. Hall and D. Blundell, *Geol. Soc. Spec. Publ.*, 106, 337–351.

Sieh, K., et al. (2008), Earthquake supercycles inferred from sea-level changes recorded in the corals of West Sumatra, *Science*, *322*, 1674–1678.

Singh, S. C., T. A. Minshull, and G. D. Spence (1993), Velocity structure of a gas hydrate reflector, *Science*, *260*, 204–207.

Singh, S. C., et al. (1998), Melt to mush variations in crustal magma properties along the ridge crest at the southern East Pacific Rise, *Nature*, *394*, 874–878.

Singh, S. C., et al. (2008), Seismic evidence for broken oceanic crust in the 2004 Sumatra earthquake epicentral region, *Nat. Geosci.*, *1*, 777–781.

Singh, S. C., S. Midenet, and Y. Djajadihardja (2009), Seismic survey of the locked and unlocked Sumatra subduction zone, *Eos Trans. AGU*, *90*(49), 471–478.

Singh, S. C., N. Hananto, A. Chauhan, H. Permana, M. Denolle, A. Hendriyana, and D. Natawidjaja (2010), Evidence of active backthrusting at the NE Margin of Mentawai Islands, SW Sumatra, *Geophys. J. Int.*, *180*, 703–714.

Subarya, C., M. Chlieh, L. Prawirodirdjo, J.-P. Avouac, Y. Bock, K. Sieh, A. Meltzner, D. Natawidjaja, and R. McCaffrey (2006), Plate-boundary deformation associated with great Sumatra-Andaman earthquake, *Nature*, *440*, 46–51.

Trehu, A., et al. (1994), Crustal architecture of the Cascadia forearc, *Science*, *266*, 237–243.

Verschuur, D. J., A. J. Berkhout, and C. Wapenaar (1992), Adaptive surface-related multiple elimination, *Geophysics*, *57*(9), 1166–1177. doi:10.1190/1.1443330.

A. P. S. Chauhan, N. D. Hananto, and S. C. Singh, Equipe de Geosciences Marines, Institut de Physique du Globe de Paris, 1 rue Jussieu, F-75238 Paris, CEDEX 05, France. (singh@ipgp.fr)